N_c and m_π dependence of ρ and σ mesons from unitarized Chiral Perturbation Theory

G. Ríos*, C. Hanhart† and J. R. Peláez*

*Departamento de Física Teórica II. Universidad Complutense de Madrid.
†Institut für Kernphysik and Jülich Center for Hadron Physics, Forschungzentrum Jülich GmbH.

Abstract. We review our work on the ρ and σ resonances derived from the Inverse Amplitude Method. In particular, we study the leading $1/N_c$ behavior of the resonances masses and widths and their evolution with changing m_π. The $1/N_c$ expansion gives a clear definition of $\bar{q}q$ states, which is neatly satisfied by the ρ but not by the σ, showing that its *dominant component* is not $\bar{q}q$. The m_π dependence of the resonance properties is relevant to connect with lattice studies. We show that our predictions compare well with some lattice results and we find that the $\rho\pi\pi$ coupling constant is m_π independent, in contrast with the $\sigma\pi\pi$ coupling, that shows a strong m_π dependence.

Keywords: Scalar mesons, chiral lagrangians, $1/N_c$ expansion
PACS: 14.40.Cs, 12.39.Fe, 13.75.Lb,11.15.Pg

Light hadron spectroscopy lies beyond the realm of perturbative QCD. At low energies, however, one can use the QCD low energy effective theory, named Chiral Perturbation Theory (ChPT) [1], to describe the dynamics of the lightest mesons. ChPT describes the interactions of the Goldstone bosons of the QCD chiral symmetry breaking, namely, the pions, by means of a effective lagrangian compatible with all QCD symmetries involving only the pion field. The infinite tower of terms in this lagrangian is organized as a low energy expansion in powers of p^2/Λ_χ^2, where p stands either for derivatives, momenta or masses, and $\Lambda_\chi \simeq 4\pi f_\pi$, where f_π denotes the pion decay constant. ChPT is renormalized order by order by absorbing loop divergences in the renormalization of higher order parameters, known as low energy constants (LECs), that parametrize the high energy QCD dynamics and *carry no energy or mass dependence*. They depend on a regularization scale μ but after renormalization the observables are independent of this scale. The value of the LECs depend on the underlying QCD dynamics and are determined from experiment. Up to the desired order, the ChPT expansion provides a *systematic and model independent* description of how observables depend on some QCD parameters like the light quark mass $\hat{m} = (m_u + m_d/2)$ or the number of colors, N_c [2].

The use of ChPT is limited to low energies and masses, nevertheless, combined with dispersion relations and elastic unitarity it leads to a successful description of meson dynamics up to energies around 1 GeV, generating resonant states not originally present in the lagrangian, without any a priori assumption on their existence or nature. In particular, we find the ρ and σ resonances as poles on the second Riemann sheet of $\pi\pi$ elastic scattering amplitudes. With this approach we can then study some of these resonances properties, like their spectroscopic nature through their mass and width dependence on N_c, or their dependence on the pion mass in order to connect with lattice studies. In the following sections we review this "unitarized ChPT" approach, named

the Inverse Amplitude Method (IAM) [3, 4, 5], and then apply it to study the leading $1/N_C$ behavior and the chiral extrapolation of the ρ and σ mesons.

The ρ and σ resonances appear as poles on the second Riemann sheet of the $(I,J) = (1,1)$ and $(I,J) = (0,0)$ $\pi\pi$ scattering partial waves of definite isospin, I and angular momentum J, respectively. Elastic unitarity implies for these partial waves, $t(s)$, and physical values of s below inelastic thresholds, that

$$\mathrm{Im}\, t(s) = \sigma(s)|t(s)|^2 \;\Rightarrow\; \mathrm{Im}\, 1/t(s) = -\sigma(s), \qquad \text{with} \quad \sigma(s) = 2p/\sqrt{s}, \tag{1}$$

where s is the Mandelstam variable and p is the center of mass momentum. Consequently, the imaginary part of $1/t$ is known exactly. However, ChPT amplitudes, being an expansion $t \simeq t_2 + t_4 + \cdots$, with $t_k = O(p^k)$, can only satisfy Eq. (1) perturbatively

$$\mathrm{Im}\, t_2(s) = 0, \quad \mathrm{Im}\, t_4(s) = \sigma(s) t_2^2(s) \quad \ldots \tag{2}$$

The resonance region lies beyond the reach of standard ChPT. This region however, can be reached combining ChPT with dispersion theory through the IAM [3, 4, 5].

The analytic structure of the $\pi\pi$ scattering amplitude $t(s)$, consisting on a right cut extending from $s_{th} = 4m_\pi^2$ to ∞, and a left cut from $-\infty$ to 0, allows to write a dispersion relation for the auxiliary function $G(s) \equiv t_2^2(s)/t(s)$

$$G(s) = G(0) + G'(0)s + \tfrac{1}{2}G''(0)s^2 + \frac{s^3}{\pi}\int_{s_{th}}^{\infty} ds' \frac{\mathrm{Im}\, G(s')}{s'^3(s'-s-i\varepsilon)} + LC(G) + PC, \tag{3}$$

where the integral over the left cut has been abbreviated as $LC(G)$ and PC stands from the pole contributions in the scalar wave corresponding to the Adler zero. The terms in Eq.(3) are evaluated using unitarity and ChPT as follows: The right cut (RC) is *exactly* evaluated considering the elastic unitarity conditions Eqs. (1), (2): $\mathrm{Im}\, G(s') = -\mathrm{Im}\, t_4(s')$. The subtraction constants only involve the amplitude and its derivatives evaluated at $s = 0$, so they can be safely approximated with ChPT: $G(0) \simeq t_2(0) - t_4(0)$, $G'(0) \simeq t_2'(0) - t_4'(0)$, $G''(0) \simeq -t_4''(0)$. The LC, being suppressed by $1/s'^3(s'-s)$, is *weighted at low energies*, so it is appropriate to approximate it with ChPT: $LC(G) \simeq -LC(t_4)$. The PC counts $O(p^6)$, it has been calculated explicitly [6] and it is numerically negligible except near the Adler zero, away from the physical region.

Neglecting PC for the moment, taking into account that $t_2(s)$ is just a first order polynomial in s, and that a dispersion relation can be also written for t_4, we can write Eq.(3) as

$$G(s) \simeq t_2(0) - t_2'(0)s - t_4(0) - t_4'(0)s - \tfrac{1}{2}t_4''(0)s^2 - RC(t_4) - LC(t_4) = t_2(s) - t_4(s), \tag{4}$$

which immediately leads to the IAM formula $t^{IAM}(s) = \frac{t_2^2(s)}{t_2(s)-t_4(s)}$. The IAM formula satisfies exact elastic unitarity and, when reexpanded at low energies, reproduces the ChPT expansion up to the order used to approximate the subtraction constants and the left cut. Here we have presented an $O(p^4)$ IAM but it can be generalized to higher chiral orders. Note that in the IAM derivation ChPT has been always used at low energies, to evaluate parts of a dispersion relation whose elastic unitarity cut has been

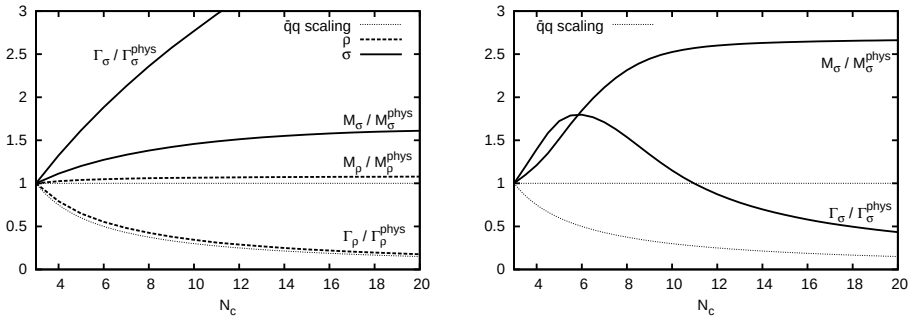

FIGURE 1. **Left:** ρ and σ $1/N_c$ scaling $O(p^4)$. **Right:** σ $1/N_c$ scaling $O(p^6)$.

taken into account exactly. Thus, there are no additional model dependencies in the approach, which is reliable up to energies where inelasticities become important. Taking the pole contribution into account leads to a modified IAM formula [6] which is almost indistinguishable from the ordinary one except in the Adler zero region, where the modified formula should be used. Actually, we use the modified IAM in this work since, as it will be shown below, one amplitude pole gets near the Adler zero region.

This simple IAM formula is able to reproduce $\pi\pi$ scattering data up to roughly 1 GeV and generates the ρ and σ poles with values of the LECs compatible with standard ChPT [5]. The $1/N_c$ expansion is implemented in ChPT through the LECs, whose leading $1/N_c$ scaling is known from QCD. Also, the m_π dependence of IAM agrees with ChPT up to the order used. Hence, it is straightforward to study the leading $1/N_C$ behavior and the $\hat{m}$ dependence of the resonances generated with the IAM.

The QCD $1/N_c$ expansion [2] provides a clear definition of $\bar{q}q$ bound states: their masses and widths scale as $O(1)$ and $O(1/N_c)$ respectively. The QCD leading $1/N_c$ behavior of the ChPT parameters (f_π, m_π and the LECs) is well known. Hence, by scaling with N_c the ChPT parameters in the IAM, the N_c dependence of the ρ and σ mesons mass and width has been determined [7, 8]. They are defined from the pole positions as $\sqrt{s_{pole}} = M - i\Gamma$. Note that we should not take too large N_C values, since the $N_c \to \infty$ is a weakly interacting limit, where the IAM approach is less reliable [9]. Also, for very large N_c, a tiny admixture of $\bar{q}q$ in the physical state could become dominant, but this does not give any information about the physical state dominant component.

Fig. 1 (left) shows the ρ and σ mass and width N_c scaling. It can be seen that the ρ follows remarkably well the expected behavior of a $\bar{q}q$ state, confirming that the method obtains the correct N_c behavior of well known $\bar{q}q$ states. In contrast,the σ does not follow that $\bar{q}q$ pattern, allowing us to conclude that its *dominant component is not* $\bar{q}q$.

Loop contributions play an important role in determining the σ pole position. Since they are $1/N_c$ suppressed compared to tree level terms, it may happen that for larger N_c they become comparable to tree level $O(p^6)$ terms, which are subdominant in the ChPT series, but not N_c suppressed. Thus we checked the $O(p^4)$ results with an $O(p^6)$ IAM calculation [8]. We defined a χ^2-like function to measure how close a resonance is from a $\bar{q}q$ behavior. First, we used it at $O(p^4)$ to show that it is not possible to find a set of LECs that makes the σ to behave predominantly as a $\bar{q}q$ state. Next, we obtained an $O(p^6)$ data fit where the ρ $\bar{q}q$ behavior was imposed. Figure 1 (right) shows the M_σ and Γ_σ N_c scaling obtained from that fit. Note that both M_σ and Γ_σ grow *near* $N_c = 3$,

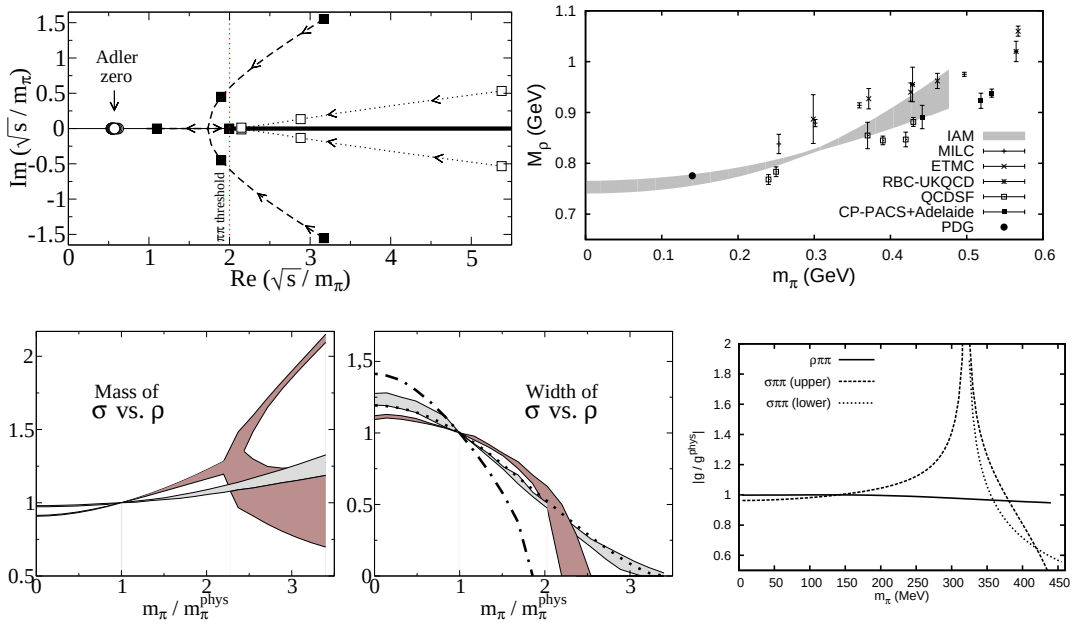

FIGURE 2. **Top Left:** Movement of the σ (dashed lines) and ρ (dotted lines) poles for increasing m_π on the second sheet. The filled (open) boxes denote the σ (ρ) pole positions at $m_\pi = 1,\ 2$, and $3 \times m_\pi^{\rm phys}$, respectively. **Top Right:** Comparison the IAM M_ρ dependence on m_π with some recent lattice results[14]. **Bottom Left:** Comparison of the ρ (light) and σ (dark) mass dependence on m_π. **Bottom Center:** Comparison of the ρ (light) and σ (dark) width dependence on m_π. The dotted (ρ) dot-dashed (σ) lines show the decrease due to only phase space assuming a constant coupling to $\pi\pi$. **Bottom Right:** ρ and σ couplings calculated from the pole residue. In all panels, the bands cover the LECs uncertainty.

confirming the $O(p^4)$ result of a non $\bar{q}q$ dominant component. However, for N_c between 8 and 15, where we still trust the IAM, M_σ becomes constant and Γ_σ starts decreasing. This may hint to a *subdominant $\bar{q}q$ component*, arising as loops become suppressed as N_c grows. Finally, by forcing the σ to behave as a $\bar{q}q$, we found that in the best case this subdominant component could become dominant around $N_c > 6-8$, but always with an $N_c \to \infty$ mass above 1 GeV instead of its physical ~ 450 MeV value. This supports the emerging picture of two low energy scalar nonets, one of exotic nature below 1 GeV and another of ordinary $\bar{q}q$ nature above 1 GeV.

ChPT also provides an expansion of m_π in terms of $\hat{m}$ (at leading order $m_\pi^2 \sim \hat{m}$). Thus, by changing m_π in the amplitudes we see how the IAM poles depend on $\hat{m}$. We report here our analysis of the ρ and σ properties dependence on m_π [10].

The values of m_π considered should fall within the ChPT applicability range and allow for some elastic regime below $K\bar{K}$, that would almost disappear if $m_\pi > 500$, which would be the most optimistic applicability range. We expect higher order corrections to be more relevant as m_π increases. Thus, our results become less reliable as m_π grows.

Fig. 2 (top left) shows the evolution of the σ and ρ pole positions as m_π is increased. In order to see the pole movements relative to the $\pi\pi$ threshold, which is also increasing, we use units of m_π, so the threshold is fixed at $\sqrt{s} = 2$. Both poles move closer to threshold and they approach the real axis. The ρ poles reach the real axis at the same time that they cross threshold. One of them jumps into the first sheet and becomes a bound state, while its conjugate partner remains on the second sheet practically at the very same position

as that in the first. In contrast, the σ poles go below threshold with a finite imaginary part before they meet in the real axis, still on the second sheet, becoming virtual states. As m_π increases, one pole moves toward threshold and jumps through the branch point to the first sheet staying in the real axis below threshold. The other σ pole moves down in energies away from threshold and remains on the second sheet. Similar movements were found within quark models [12] and a finite density analysis [13].

Fig. 2 (top right) shows our results for M_ρ dependence on m_π compared with some lattice results [14] and the M_ρ PDG value. In view of the incompatibilities between different lattice collaborations, we find a qualitative good agreement with lattice results. The M_ρ dependence on m_π agrees also with estimations for the two first coefficients of its chiral expansion [15].

In Fig. 2 (bottom left) we compare the m_π dependence of M_ρ and M_σ, normalized to their physical values. The bands cover the LECs uncertainties. Both masses grow with m_π, but M_σ grows faster than M_ρ. Above $2.4\, m_\pi^{\text{phys}}$, we show two bands since the two σ poles lie on the real axis with two different masses.

In the bottom center panel of Fig. 2 we compare the m_π dependence of Γ_ρ and Γ_σ normalized to their physical values: note that both widths become smaller. We compare this decrease with the expected phase space reduction as resonances approach the $\pi\pi$ threshold. We find that Γ_ρ follows very well this expected behavior, which implies that the $\rho\pi\pi$ coupling is almost m_π independent. In contrast, Γ_σ deviates from the phase space reduction expectation. This suggests a strong m_π dependence of the σ coupling to two pions, which we confirm with a explicit calculation of the resonances couplings from the pole residues as shown in the bottom left panel.

REFERENCES

1. S. Weinberg, Physica **A96** (1979) 327. J. Gasser and H. Leutwyler, Annals Phys. **158** (1984) 142;
2. G. 't Hooft, Nucl. Phys. B **72**, 461 (1974). E. Witten, Annals Phys. **128**, 363 (1980).
3. T. N. Truong, Phys. Rev. Lett. **61** (1988) 2526. Phys. Rev. Lett. **67**, (1991) 2260; A. Dobado et al., Phys. Lett. **B235** (1990) 134.
4. A. Dobado and J. R. Peláez, Phys. Rev. D **47** (1993) 4883; Phys. Rev. D **56** (1997) 3057.
5. F. Guerrero and J. A. Oller, Nucl. Phys. B **537** (1999) 459 [Erratum-ibid. B **602** (2001) 641]. J. R. Peláez, Mod. Phys. Lett. A **19**, 2879 (2004) A. Gómez Nicola and J. R. Peláez, Phys. Rev. D **65** (2002) 054009 and AIP Conf. Proc. **660** (2003) 102.
6. A. Gómez Nicola, J.R. Peláez and G. Ríos, Phys. Rev. D **77** (2008) 056006.
7. J. R. Pelaez, Phys. Rev. Lett. **92**, 102001 (2004)
8. J. R. Pelaez and G. Rios, Phys. Rev. Lett. **97**, 242002 (2006)
9. J. R. Pelaez and G. Rios, arXiv:0905.4689 [hep-ph].
10. C. Hanhart, J. R. Pelaez and G. Rios, Phys. Rev. Lett. **100**, 152001 (2008)
11. D. Morgan, Nucl. Phys. A **543** (1992) 632; D. Morgan and M. R. Pennington, Phys. Rev. D **48** (1993) 1185.
12. E. van Beveren et al., AIP Conf. Proc. **660**, 353 (2003); Phys. Rev. D **74**, 037501 (2006).
13. D. Fernandez-Fraile, A. Gomez Nicola and E. T. Herruzo, Phys. Rev. D **76**, 085020 (2007)
14. Ph. Boucaud *et al.* [ETM Collaboration], Phys. Lett. B **650**, 304 (2007) C. Allton *et al.* [RBC and UKQCD Collaborations], Phys. Rev. D **76**, 014504 (2007) C. W. Bernard *et al.*,Phys. Rev. D **64**, 054506 (2001) C. R. Allton *et al.*Phys. Lett. B **628**, 125 (2005) M. Gockeler *et al.*[QCDSF Collaboration], [arXiv:hep-lat/0810.5337].
15. P. C. Bruns and U.-G. Meißner, Eur. Phys. J. C **40** (2005) 97.